Nuclear Inclusion of Nontargeted and Chromatin-Targeted Polystyrene Beads and Plasmid DNA Containing Nanoparticles

ARTICLE *in* MOLECULAR PHARMACEUTICS · AUGUST 2011

Impact Factor: 4.38 · DOI: 10.1021/mp200120v · Source: PubMed

6 AUTHORS, INCLUDING:

Nathalie Symens
ISMS Belgium
11 PUBLICATIONS **82** CITATIONS
SEE PROFILE

Jo Demeester
Ghent University
240 PUBLICATIONS **8,746** CITATIONS
SEE PROFILE

Stefaan De Smedt
Ghent University
329 PUBLICATIONS **11,286** CITATIONS
SEE PROFILE

Katrien Remaut
Ghent University
52 PUBLICATIONS **841** CITATIONS
SEE PROFILE

molecular pharmaceutics

ARTICLE

pubs.acs.org/molecularpharmaceutics

Nuclear Inclusion of Nontargeted and Chromatin-Targeted Polystyrene Beads and Plasmid DNA Containing Nanoparticles

Nathalie Symens,[†] Rudolf Walczak,[‡] Joseph Demeester,[†] Iain Mattaj,[‡] Stefaan C. De Smedt,[†] and Katrien Remaut*,[†]

[†]Laboratory of General Biochemistry and Physical Pharmacy (Ghent Research Group on Nanomedicines), Faculty of Pharmaceutical Sciences, Ghent University, Harelbekestraat 72, 9000 Ghent, Belgium

[‡]Directors' Research, Mattaj Group, European Molecular Biology Laboratory, Meyerhofstraße 1, 69117 Heidelberg, Germany

ABSTRACT: The nuclear membrane is one of the major cellular barriers in the delivery of plasmid DNA (pDNA). Cell division has a positive influence on the expression efficiency since, at the end of mitosis, pDNA or pDNA containing complexes near the chromatin are probably included by a random process in the nuclei of the daughter cells. However, very little is known about the nuclear inclusion of nanoparticles during cell division. Using the *Xenopus* nuclear envelope reassembly (XNER) assay, we found that the nuclear enclosure of nanoparticles was dependent on size (with 100 and 200 nm particles being better included than the 500 nm ones) and charge (with positively charged particles being better included than negatively charged or polyethyleneglycolated (PEGylated) ones) of the beads. Also, coupling chromatin-targeting peptides to the polystyrene beads or pDNA complexes improved their inclusion by 2- to 3-fold. Upon microinjection in living HeLa cells, however, nanoparticles were never observed in the nuclei of cells postdivision but accumulated in a specific perinuclear region, which was identified as the lysosomal compartment. This indicates that nanoparticles can end up in the lysosomes even when they were not delivered through endocytosis. To elucidate if the chromatin binding peptides also have potential in living cells, this additional barrier first has to be tackled, since it prevents free particles from being present near the chromatin at the moment of cell division.

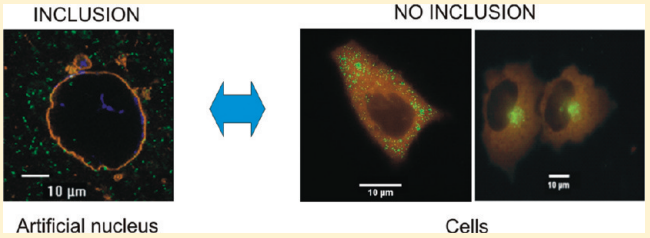

KEYWORDS: cell division, nuclear enclosure, *Xenopus laevis*, HeLa cells, pDNA delivery, nuclear exclusion, mitosis, nuclear envelope reassembly

INTRODUCTION

Gene therapy shows potential in the treatment of a wide variety of genetic disorders. For gene therapy to be successful, the nucleic acids should reach their target, which is situated intracellularly. Naked nucleic acids are poorly taken up by cells. Therefore, they are administered by using viral or nonviral vectors. In general, viral vectors provide high transfection efficiencies but suffer from the limited amount and size of the genetic material they can carry. Also, they can induce severe immune responses. Nonviral vectors are advantageous over viral vectors in that they are less expensive, easier and safer to make and more suitable for long term storage. They can also deliver much larger pieces of DNA when compared to viral methods.[1] Nonviral vectors mostly enter the cells by endocytosis. Then, they have to escape from the endosomal compartment and release their therapeutic DNA in the cytoplasm of the cells. Furthermore, the therapeutic DNA should stay intact and reach its target, which is the nucleus in the case of plasmid DNA (pDNA). Plasmid DNA delivery and expression remain challenging despite many years of nonviral gene therapy research. Although nonviral systems have many advantages, their expression efficiency is very low when compared to viral systems. Factors which decrease expression efficiency include cytoplasmic sequestration (by interactions with DNA binding proteins and cytoskeletal elements),[2,3] enzymatic degradation,[4] decomplexation from carrier molecules[5] and, most importantly, lack of transport across the nuclear membrane, which is one of the major cellular barriers.[6,7] In nondividing cells, the transfer through the nuclear pore complexes (NPCs) of intact nuclear envelopes is very inefficient. Many studies suggest that although it is not impossible, larger molecules such as pDNA do not readily cross NPCs.[2,8−11] Several attempts at improving nonviral entry of pDNA into the nucleus have been published, in which nuclear localization signal (NLS) containing proteins or peptides were attached to the pDNA by electrostatic interactions[12] or covalent binding.[13] Also, attachment to cellular DNA binding proteins including histones[14] and high-mobility group (HMG) proteins,[15] as well as DNA containing the Simian Virus 40 (SV40) promoter and origin of replication,[16] has been investigated. These attempts at improving the transport of DNA to the nucleus have however met with limited success.

Interestingly, several groups have observed that the expression efficiencies of cationic lipid-, polymer- and peptide-based transfection reagents were two- to several hundred-fold higher in dividing as compared to nondividing cells.[9,11,17−24] Also, cell

Received: March 11, 2011
Accepted: August 14, 2011
Revised: August 8, 2011
Published: August 22, 2011

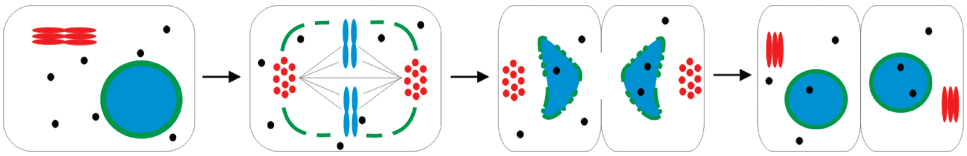

Figure 1. Principle of nuclear inclusion during cell division. (Black) nanoparticles, (green) nuclear membrane, (red) Golgi apparatus and (blue) chromatin.

division had a positive influence on the nuclear inclusion of colloidal gold particles.[25] This suggests that transfection close to M phase is perhaps facilitated by nuclear membrane breakdown, since the disassembly of the nuclear envelope during cell division most likely facilitates access to the nucleoplasm and chromatin. It is plausible that the naked pDNA or nanoparticles near the chromatin are included by chance in the nuclei of the daughter cells during mitosis, as is presented in Figure 1.

Previous studies which focused on the fate of nanoparticles and the dependence of their characteristics in living cells mostly delivered the nanoparticles through uptake by endocytosis. It was reported, for example, that the pathway of internalization depends on the size of the polystyrene nanoparticles.[26] Furthermore, the uptake mechanism, uptake rate, cytotoxicity and exocytosis of gold nanoparticles of different size and shape were investigated.[27,28] Recently, Errington and colleagues studied the fate of nanoparticles during the cell cycle. The quantum dots were asymmetrically and nonrandomly diluted over daughter cells, which is probably related to a survival mechanism of the cell responding to stress.[29] Although the nuclear inclusion appears a very simple concept to study, very little is known on the nuclear entry of nanoparticles during cell division. How and to what extent can nanoparticles access the nucleoplasm during cell division? Is nuclear inclusion random, or do nanoparticles need to interact with chromatin to be enclosed? Do the nanoparticles remain in the nucleoplasm during subsequent cell cycles? Many of these questions remain unanswered, although they are highly relevant for nonviral gene delivery. We addressed these open questions by studying to which extent nanoparticles are enclosed in artificial *Xenopus laevis* nuclei and in daughter nuclei of dividing HeLa cells. The *Xenopus* nuclear envelope reassembly (XNER assay) functions as a model system, in which the enclosure of nanoparticles in fully functional artificial nuclei can be studied in the most ideal situation, e.g. without the presence of additional extracellular and intracellular barriers. In case of the HeLa cells the nanoparticles were microinjected into the cytosol so as to avoid additional intracellular barriers such as cellular uptake and endosomal escape, and to prevent trapping of particles inside endosomes through endocytic uptake. We investigated whether the size and charge of the nanoparticles had an influence on the nuclear inclusion and if the enclosure could be enhanced by modification of the nanoparticles by using chromatin binding peptides since one might expect more efficient enclosure by binding to the chromatin during cell division.

MATERIAL AND METHODS

Polystyrene Beads. Green fluorescent carboxylated polystyrene beads (Molecular Probes) of different size (100, 200, and 500 nm) were used. These beads have a negative ζ-potential and were modified with Pluronic F-127 (Sigma-Aldrich) and dimethylamine−ethylamine (DMAEA) to obtain respectively polyethyleneglycolated (PEGylated)[30] and positively charged beads (see Table 1). The latter is the result of an amide formation between the carboxylate groups on the beads and the amine group of DMAEA. The carboxylate groups were activated with an excess of EDC at pH 5. DMAEA (at pH 5) was added, and this was shaken overnight. Then, Microcon-YM-100 (Millipore) columns were used to purify the positively charged beads. These series of beads are called "nontargeted beads". Additionally, the carboxylated 100 nm beads were modified via a NH_2-PEG-maleimide linker with 3 gluthatione *S*-transferase (GST)-tagged peptides, namely, Mel-28, mutated Mel-28 or HMGA2β (Figure 2A). Briefly, 10 mg/mL NH_2-PEG-maleimide (creative PEGworks) was added to 500 μL of 0.4% solution of the carboxylated beads and incubated overnight at 4 °C. Then, the beads were purified by centrifugation over Microcon-YM-100 columns and re-collected after 2 washing steps by reversed centrifugation. The modified beads were incubated overnight with 50 μg of GST-tagged proteins to allow binding to the maleimide side of the NH_2-PEG-maleimide linker. The beads were again purified by centrifugation over Microcon-YM-100 columns and re-collected after 2 washing steps by reversed centrifugation. Further on, these beads are called "targeted beads". Mel-28, mutated Mel-28 and HMGA2β were prepared as described elsewhere.[31] Diameter and ζ-potential measurements of the nontargeted beads were done with a ZETASIZER NANO (Malvern Instruments).

pDNA/PEI Polyplexes. As pDNA nanoparticles we made use of pDNA complexed to 7.5 kDa linear polyethyleneimine (PEI) (kindly provided to us by Olivia Merkel, Marburg University, Germany). For targeting and microinjection experiments, pDNA was labeled with Cy5 (fluorescent red) using the *Label* IT Cy5 labeling kit (Mirus Bio Corporation) and purified by purification columns as supplied by the manufacturer. Complexes were prepared by adding a PEI polymer solution to an equal volume of a 0.04 μg/μL pDNA solution to obtain a nitrogen to phosphate ratio (N/P ratio) of 10, followed by vortexing the dispersion for 10 s, and were allowed to equilibrate at room temperature for 30 min prior to use. To obtain targeted pDNA/PEI nanoparticles, complexes were prepared with PEI polymers which were modified with peptides of Mel-28, mutated Mel-28, or HMGA2β through a NHS-PEG-maleimide linker. Briefly, 1 mg/mL PEI polymer solution was incubated with 10 times excess of NHS-PEG-maleimide (Pierce, Thermo Scientific) and purified by a Zeba Desalt spin column (Thermo scientific) after 4 h of incubation at room temperature. Then, 220 μL of the partially modified PEI polymers was incubated overnight at 4 °C with 13.5 μg of GST-tagged peptides to allow binding to the maleimide side of the NHS-PEG-maleimide linker so that chromatin targeted PEI polymers were obtained. In this concentration, almost all GST-tagged peptides bound to the PEI polymers, which makes further purification unnecessary. To be sure, however, the PEI complexes were additionally purified by centrifugation over Microcon-YM-100 columns and re-collected after 2 washing steps by reversed centrifugation before use. The diameter and ζ-potential of the nontargeted and targeted pDNA/PEI

Table 1. Mean Diameter (nm) and ζ-Potential (mV) of the Positively Charged (pos), PEGylated (PEG) and Negatively Charged (neg) Polystyrene Beads and of pDNA/PEI Complexes Made with Nonmodified PEI and PEI Modified with Mel-28, Mutated Mel-28 and HMGA2β[a]

	500 nm beads			200 nm beads			100 nm beads			pDNA/PEI complexes			
	neg	PEG	pos	neg	PEG	pos	neg	PEG	pos	nontargeted	Mel-28	mut	HMGA2β
size (nm)	577 ± 4	608 ± 10	589 ± 3	233 ± 1	249 ± 2	248 ± 2	116 ± 1	134 ± 1	122 ± 2	168 ± 10	131 ± 6	154 ± 7	238 ± 6
ζ (mV)	−52 ± 1	−29 ± 1	26 ± 1	−47 ± 1	−30 ± 1	26 ± 1	−45 ± 2	−23 ± 1	29 ± 1	29 ± 3	21 ± 2	22 ± 2	17 ± 2

[a] The given standard deviations are the result of repeated measurements.

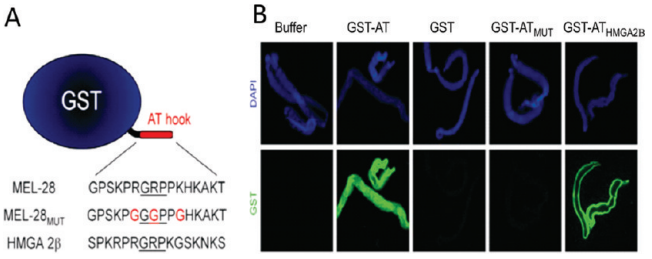

Figure 2. Sequence (A) and *in vitro* chromatin-targeting properties (B) of Mel-28 (GST-AT), GST alone, mutated Mel-28 (GST-AT_{MUT}) and HMGA2β (GST-$AT_{HMGA2β}$). Only Mel-28 and HMGA2β target to the chromatin (stained blue with DAPI, upper panel), as can be concluded from the green immunostaining against GST (lower panel).

polyplexes were measured with a ZETASIZER NANO (Malvern Instruments).

Immunostaining of GST-AT-hooks. The initial chromatin binding properties of Mel-28, mutated Mel-28 and HMGA2β were evaluated with immunostaining against the GST-fragment of the AT-hooks. Membrane-free extract was supplemented with GST alone or GST-AT-hooks at 1 μM final concentration, and incubated with chromatin for 10 min. Then, the chromatin was fixed with 4% PFA in PBS for 10 min. The fixed chromatin was placed on top of 0.8 mL 30% sucrose cushion in PBS and centrifuged onto poly-L-lysine coated coverslips. Blocking was carried out for 30 min in 1% BSA-PBS. Then, the samples were incubated with the primary anti-GST antibody in 1% BSA-PBS for 2 h, followed by extensive washing before the fluorescein-labeled secondary antibody (in 1% BSA-PBS) was added for 1 h. After washing, the chromatin was stained by adding 0.1 μg/mL DAPI and the samples were visualized with a fluorescence microscope.

***Xenopus* Nuclear Envelope Reassembly (XNER) Assay.** Cytosolic extract and membrane fraction needed for the XNER assay were isolated from *Xenopus laevis* eggs, and sperm chromatin was prepared from *Xenopus leavis* sperm (*Xenopus laevis* testes were kindly provided by Kris Vleminckx Lab, VIB, Ghent) as previously described by Hetzer et al. (2000).[32] To study the nuclear inclusion in the XNER assay, 1 μL of polystyrene beads (green) or Cy5-pDNA/PEI nanoparticles (red) was added to a mixture of sperm chromatin (0.6 μL) and cytosolic extract (20 μL) and incubated in a water bath at 20 °C for 20 min. Then, 1 μL of membrane fraction, 1 μL of energy mix (127.5 mg/mL creatin phosphate, 2.5 mg/mL creatin kinase, 25 mM ATP and 25 mM GTP) and 1 μL of glycogen (200 mg/mL) were added, and this mixture was incubated in a water bath at 20 °C to allow the formation of artificial nuclei as described by Hetzer et al. (2000).[32] After 90 min the artificial nuclei were stained with $DiIC_{18}$ (membrane staining) and DAPI (chromatin staining) and the enclosure of the nanoparticles in the nuclei was visualized with a Nikon EZC1-si (Nikon Belux, Brussels, Belgium) by fluorescence confocal laser scanning microscopy (CLSM) or epifluorescence microscopy. The particles were counted by moving up and down the *Z*-focus to visualize the artificial nuclei in 3-D. It should be noted that in the case of 100 and 200 nm particles, because of the diffraction limit, an underestimation of the amount of particles is possible when aggregates are counted as one. However, the effect of chromatin targeting is compared to its control situation, in which the same error is expected to occur.

Microinjection of HeLa Cells. HeLa cells (human epithelial cervical cancer cells, ATCC number: CCL-2) were cultured in Dulbecco's modified Eagle's medium: nutrient mixture F-12 (DMEM-F12) (Gibco) containing 2 mM glutamine, 10% heat inactivated fetal bovine serum (Hyclone/Perbio) and 100 U/mL penicillin−streptomycin liquid (Gibco) at 37 °C in a humidified atmosphere containing 5% CO_2. For microinjection experiments, HeLa cells (2.5×10^4 cells/cm^2) were plated onto sterile glass bottom culture dishes (MatTek Corporation) and allowed to adhere for 1 day. Microinjection with the polystyrene beads (green or red) or Cy5-pDNA/PEI nanoparticles (red) was performed with a Femtojet microinjector and an Injectman NI 2 micromanipulator (Eppendorf) mounted on a Nikon EZC1-si confocal laser scanning microscope. Injections were performed in the cytoplasm, using polystyrene beads or pDNA/PEI complexes in HEPES buffer. Injection solutions were supplemented with 2 mg/mL 70 kDa TRITC−dextran (Sigma-Aldrich) to identify the place of injection and cell division. After microinjection, cells were put back into the incubator and fluorescence microscopy images were taken 30 min and 24 h after injection. Labeling of the lysosomes was performed by adding 1 μL of Lysosensor green (Invitrogen) to the microinjected cells. Labeling of the endosomes was performed by transfecting the cells with CellLight Early Endosomes-GFP BacMam 2.0 (Invitrogen). Colocalization of injected fluorescent red beads with the labeled cell compartments was analyzed using Image J (http://rsbweb.nih.gov/ij/).

RESULTS

Characteristics of Nontargeted and Targeted Nanoparticles. As nontargeted nanoparticles, we made use of polystyrene beads of 100, 200, and 500 nm as this is the size range in which most of the nonviral gene delivery complexes are situated. Initially, also polystyrene beads of 20 and 40 nm were included in the study, as model particles that should be able to cross the NPCs. However, due to problems of functionalization, aggregation and detection of these weakly fluorescent particles, these smaller particles were omitted from further study.

First, the carboxylated polystyrene beads, as bought from the manufacturer, were functionalized to obtain positively charged or

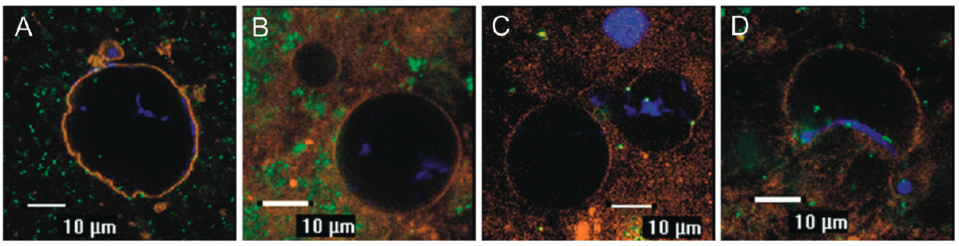

Figure 3. Representative confocal fluorescence images of the limited nuclear enclosure of nontargeted beads (100 nm, positively charged [A]; 200 nm, positively charged [B]; 500 nm, positively charged [C]) and chromatin-targeted beads (100 nm, HMGA2β [D]) in artificial *Xenopus* nuclei. Blue: sperm chromatin. Orange: membrane fraction. Green: polystyrene beads. Only fully decondensed nuclei (>25 μm) were counted.

PEGylated beads. In Table 1, the mean diameter (nm) and ζ-potential (mV) of these different kinds of nanoparticles are presented. It can be seen that, for a given size, the negatively charged beads are always slighty larger than stated by the manufacturer. Also, making the beads positively charged or PEGylated results in a further size increase. The ζ-potential demonstrates that we indeed succeeded in making positively charged particles. In the case of PEGylated particles, the ζ-potential becomes less negative due to the presence of the PEG chains.

Apart from polystyrene beads, also pDNA/PEI nanoparticles were used as a model for nonviral gene delivery vehicles. PEI was chosen as complexation partner for the pDNA to form pDNA/PEI polyplexes as it is a well-characterized polymer for gene delivery which is hypothesized to be able to enter the nucleus during transfection.[33] To obtain chromatin-targeted nanoparticles, both the 100 nm beads and the pDNA/PEI polyplexes were modified with chromatin binding peptides. As chromatin targeting peptides, part of the proteins Mel-28, mutated Mel-28 or HMGA2β were chosen. These peptides contain an AT-hook, a DNA binding motif found in a family of proteins that binds the minor groove of the AT-rich scaffold-associated regions (SARs) on metaphase chromosomes.[34] Mel-28 is associated with two types of structures in the cell, one implicated in nuclear envelope function and the other in chromatin organization, and is recruited to chromatin at an early time point during nuclear assembly.[35,36] HMGA2β is a small non-histone chromatin-associated protein that belongs to the family of the HMG proteins, architectural factors which regulate the chromatin structure by specifically binding and bending the DNA and creating active and inactive chromatin regions which are essential for gene expression.[37−39] Figure 2A shows the sequences of the AT-hooks which were used. The specific targeting of Mel-28 (GST-AT) and HMGA2β (GST-$AT_{HMGA2\beta}$) to the chromatin can be seen after immunostaining of the GST-fragment of the chromatin targeting peptides (Figure 2B), while GST alone, or GST-tagged mutated Mel-28 (GST-AT_{MUT}), does not stain the chromatin. Table 1 also contains the mean diameter (nm) and ζ-potential (mV) of the pDNA/PEI polyplexes before and after functionalization with the chromatin targeting peptides. It can be seen that the charge of the functionalized polyplexes slightly decreases, while the size slightly decreases for Mel28 and mutated Mel28, but increases for HMGA2β. Due to the small sample volume and cost of material, the diameter and ζ-potential of the targeted beads could not be measured.

Nuclear Inclusion of Nontargeted Polystyrene Beads with Different Size/Charge in the XNER Assay. The artificial nuclei (Figure 3) are obtained with the *Xenopus* nuclear envelope reassembly (XNER) assay. In this assay, sperm chromatin is first mixed with cytosolic extract, which results in a partial decondensation of the sperm chromatin. It should be noted that *Xenopus* sperm chromatin is much more compact than normal mitotic chromatin but is spontaneously repackaged with histones in the cytosolic extract to become normal mitotic chromatin.[40−44] Then, upon the addition of membrane extract and an ATP generating buffer, the membrane fractions bind to the chromatin and eventually fuse so that nuclear membranes are formed around the chromatin material. Then, the chromatin decondenses further and nuclear proteins are imported, resulting in the swelling of the nuclei so that functional artificial nuclei are formed.[40,41,43−46] By addition of fluorescently labeled nanoparticles to the XNER assay, we could evaluate the efficiency with which different types of nanoparticles are entrapped in the formed nuclei.

Figure 3 shows representative examples of artificial nuclei obtained with the XNER assay. Depending on where in the sample the pictures are taken, more or fewer membrane elements or beads seem to be present, although the total number of particles and membrane elements in each situation is comparable. Also, only fully decondensed nuclei (>25 μm) were counted as the smaller ones represent unfinished nuclei and should not be taken into account. Between 50 and 100 of these large, functional nuclei were analyzed for each experiment with a different type of nanoparticle. The results are summarized in Figure 4 showing the percentage of nuclei containing 0, between 1 and 5, between 6 and 10, or more than 10 nanoparticles. It can be seen, in Figure 3 as well as in Figure 4, that from time to time the nontargeted beads are enclosed in the artificial nuclei but enclosure is rather limited. Nevertheless, size and charge do have an influence on nuclear entry (Figure 4). The enclosure of the positively charged beads is higher than the enclosure of the negatively charged or the PEGylated ones. Apart from the charge, it can be seen that also size matters: beads with a diameter of 200 and 100 nm were better enclosed than the 500 nm ones. Thus, the diameter, volume and/or weight can impair the inclusion. We conclude that small (100−200 nm) positively charged beads have the best chance to be retained in the nucleus upon cell division.

Nuclear Inclusion of Chromatin-Targeted Polystyrene Beads and pDNA/PEI Complexes in the XNER Assay. In these experiments, not only the inclusion in the artificial nuclei but also the initial binding to chromatin before adding the membrane fraction to the XNER assay was determined. Figure 5A shows that the enclosure of beads modified with the chromatin binding peptides derived from Mel-28 or HMGA2β is indeed higher than the enclosure of the best nontargeted beads (100 nm, positively charged) and the beads modified with the mutated AT-hook (Mel-28 mut), showing the potential of chromatin targeting. To verify if chromatin targeting also had an influence on pDNA complexes used in nonviral gene delivery, red labeled pDNA/PEI polyplexes were added to the XNER assay and their chromatin

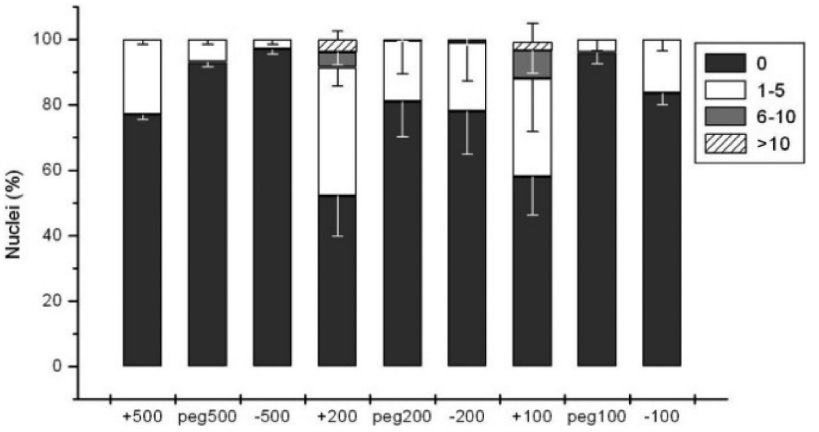

Figure 4. Enclosure of nontargeted polystyrene beads of different size (500, 200, or 100 nm) and ζ-potential (positive, PEGylated or negative) in artificial *Xenopus* nuclei. The percentage of nuclei (as denoted in the *y*-axis) containing 0, 1−5, 6−10 and >10 beads is shown. Only fully decondensed nuclei (>25 μm) were counted. The error bars come out of at least 3 independent experiments where 50 to 100 nuclei were counted per experiment. Half of the corresponding error bars are presented for preventing overlap, respectively in the directions minus, minus, minus and plus.

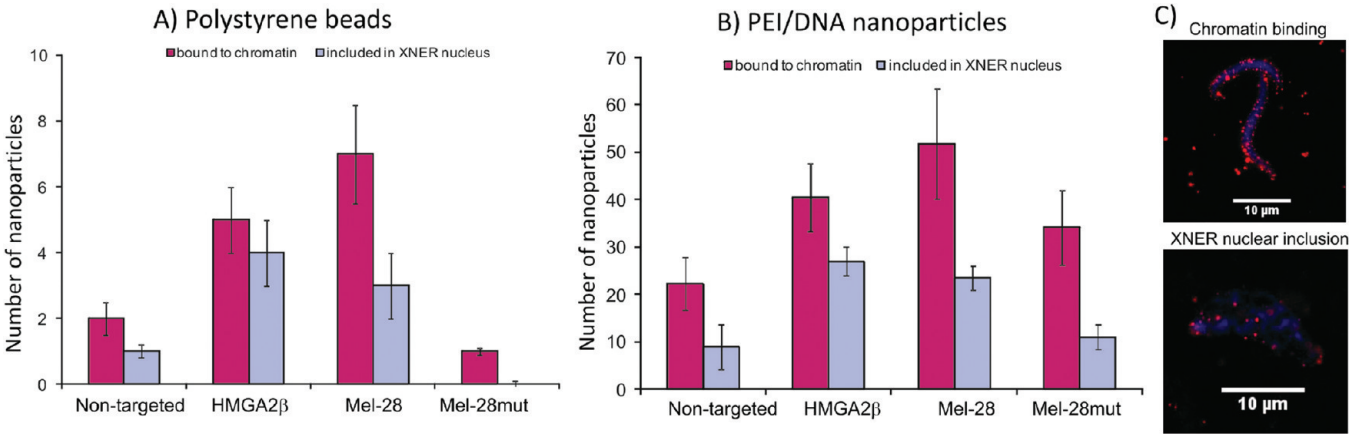

Figure 5. Average number of particles per chromatin strand (purple bars) and average number of particles per artificial nucleus (blue bars) with nontargeted (positively charged) and targeted 100 nm polystyrene beads (A) or 7.5 kDa linear pDNA/PEI complexes (B). Between 25 and 50 chromatin strands and artificial nuclei were counted. A 2−3-fold targeting when compared to nontargeted beads or polyplexes can be observed. The microscopy images (C) show a representative picture of pDNA/PEI complexes (red) bound to the chromatin (blue) or included in the XNER nuclei.

binding and nuclear inclusion was visualized (Figure 5B). Also here, the use of chromatin-targeting AT-hooks Mel-28 and HMGA2β resulted in a 2- to 3-fold increase in nanoparticles which were included in the artificial nuclei. Thus, targeting to the chromatin can indeed enhance the nuclear inclusion, although it should be noted that not all particles initially bound to the chromatin get included in the artificial nuclei (Figure 5A−C). Assuming that one chromatin strand leads to the formation of one artificial nucleus, HMGA2β-targeted particles are the most resistant to displacement, since respectively about 45%, 75%, 45% and 30% of the initially chromatin-bound particles are included in the eventually formed artificial nuclei in the case of nontargeted, HMGA2β, Mel-28 and mutated Mel-28 modified nanoparticles.

Nuclear Inclusion of Microinjected Polystyrene Beads and pDNA/PEI Polyplexes in HeLa Cells. We were interested to see whether polystyrene beads (100 nm) and pDNA/PEI complexes which are present in the cytoplasm gain access to the nucleus during cell division. Since Figure 5A and Figure 5B show that even for nontargeted positively charged nanoparticles about 45% of the particles which bind to chromatin are retained in the formed nuclei, we would expect to find at least some chromatin binding particles in the nuclei of the daughter cells. To circumvent endocytosis and the need for endosomal escape, the nontargeted nanoparticles were delivered by directly injecting them into the cytoplasm of HeLa cells. Injection solutions were supplemented with TRITC−dextran to identify the place of injection and whether or not injected cells divide. Figure 6 shows representative images of the intracellular distribution of 100 nm positively charged polystyrene beads (green) and pDNA/PEI polyplexes (red) during cell division, in injected living HeLa cells. Initially, the polystyrene beads spread through the cytoplasm, while the pDNA/PEI complexes remained closer to the place of injection (indicated by an arrow). Also, the pDNA/PEI complexes can be seen to "line up" at the nuclear membrane, demonstrating that they are not "pushed" through the NPCs by the applied injection pressure. Upon cell division, it can be seen that both the polystyrene beads and the pDNA/PEI complexes are evenly distributed over the two daughter cells, but accumulate in the perinuclear region of the daughter cells, rather than being present in the

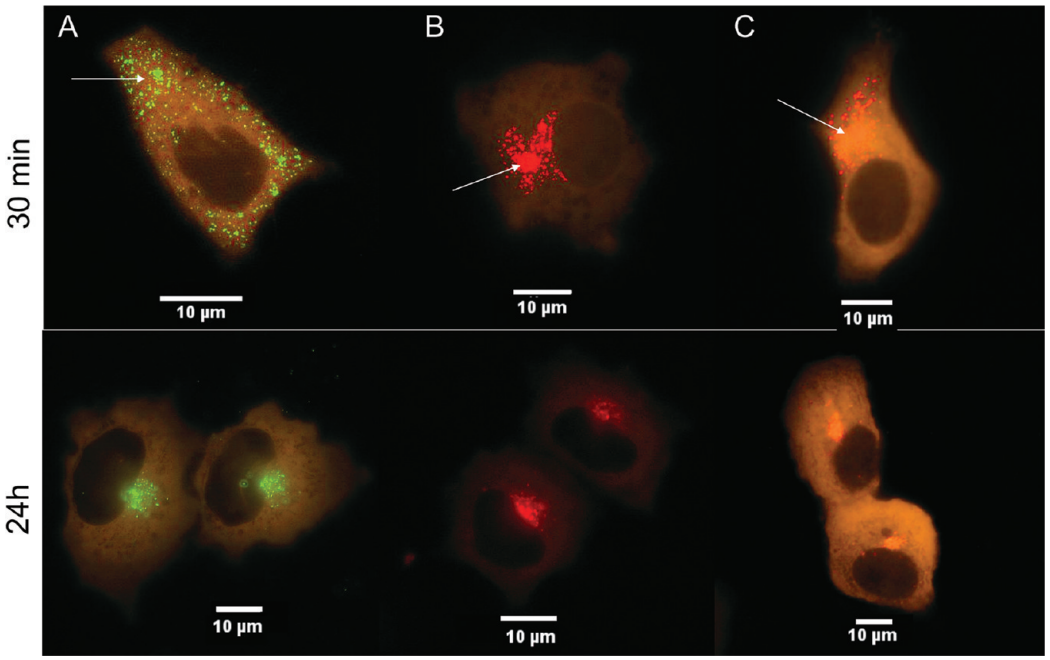

Figure 6. Intracellular distribution upon microinjection of nanoparticles in HeLa cells. (A) Polystyrene beads (100 nm, positively charged, green), (B) pDNA/PEI polyplexes (about 170 nm, positively charged, red), (C) pDNA/PEI-HMGA2β polyplexes (about 240 nm, positively charged, red) and 70 kDa TRITC−dextran (orange) as a coinjection marker. Pictures of the injected cells were taken 30 min and 24 h after injection. An arrow indicates the initial place of injection.

nuclei of these cells. Indeed, enclosure of nanoparticles in the nuclei of cells which had undergone division was never observed. This is in contrast to the nuclear inclusion seen in assembled nuclei in the XNER assay, where there were about 10 pDNA/PEI complexes present in the case of nontargeted complexes (see Figure 5B). Apart from nontargeted nanoparticles, also nanoparticles targeted with HMGA2β were used for microinjection (Figure 6C). HMGA2β was chosen as the data in Figure 5 pointed out that, in this case, the largest fraction of chromatin-bound nanoparticles is retained in the formed nuclei. Also here, however, the nanoparticles were never observed in the nuclei of divided cells, but again accumulated in this specific perinuclear region. Whether the nanoparticles first reach the nuclear interior and are then expelled to this perinuclear region, or accumulate in this perinuclear region already before cell division occurs, is not clear.

Identification of the Specific Perinuclear Region Where Nanoparticles Tend To Accumulate. Since we found that the injected polystyrene beads or pDNA/PEI complexes both accumulate in a specific perinuclear region, we were interested to determine what this perinuclear region could be. Therefore, we performed staining of cell compartments such as the early endosomes and the lysosomes. To prevent overlap between the staining color and the injected beads, red fluorescent beads were injected instead of green ones. Colocalization of the red and the green channel was determined in Image J after a background subtract, so that colocalized pixels appear white, while noncolocalized pixels appear green or red in the overlay image. Figure 7A shows that there is no colocalization between the injected beads and the early endosomes: no white pixels are found in the colocalization image. When the lysosomes were stained, however, a great amount of colocalization was observed after 24 h of incubation (Figure 7C). This is an interesting observation which implies that nanoparticles can end up in the lysosomal compartment even when they are directly injected in the cytoplasm and not taken up by endocytosis. When the colocalization with the lysosomes was evaluated immediately after injection, no colocalization was found (Figure 7B), indicating that the colocalization observed after 24 h is not an artifact, but indeed results from the accumulation of the injected nanoparticles in the lysosomal compartment. It should be noted that, when performing microinjections, there is a constant flow of nanoparticles from the injection needle. Therefore, one could argue that the nanoparticles in the surrounding environment can be taken up by endocytosis and end up in the lysosomes in this way. It can be seen, however, that mainly the injected cells contain the nanoparticles, showing that the endocytosis of free nanoparticles in the medium is negligible.

DISCUSSION

What happens with nanoparticles during cell division is a highly relevant question in gene delivery, with regard to both biological activity and toxicity issues.[47] Most studies focusing on the intracellular fate of molecules during cell division are however performed with macromolecules such as free pDNA or dextrans or with smaller gold particles (30−170 Å).[25] The nuclear inclusion of larger nanoparticles, such as those used in this study, has not previously been systematically studied in either cell-free systems or living cells. In living cell experiments, this can partially be explained by the difficulties to inject particles which are larger than 200 nm because of problems of aggregation, needle clogging and long-term survival of the cells after injection. Using the cell-free XNER assay (which is the only way to isolate the process of nuclear inclusion), however, we were able to investigate the influence of size and charge of nanoparticles on their nuclear inclusion and found that 100 or 200 nm particles were more efficiently included than those of 500 nm. We hypothesize that

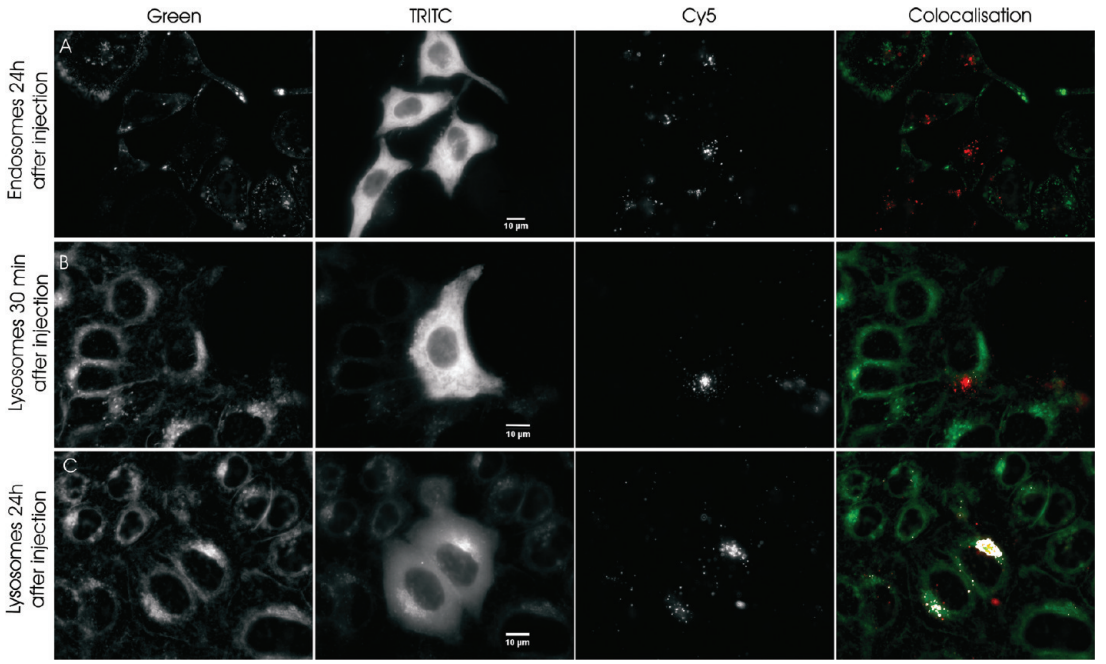

Figure 7. Identification of the perinuclear region upon microinjection of red polystyrene beads in HeLa cells. 70 kDa TRITC−dextran was used as a coinjection marker. Pictures of the injected cells were taken 30 min (B) or 24 h (A, C) after injection. The green panel shows the labeling of the endosomes (A) or the lysosomes (B and C). The TRITC panel shows the injected (divided in C) cells, while the Cy5 panel shows the injected red beads. Colocalization of the red beads with the green endosomes or lysosomes was evaluated using Image J. Colocalized pixels appear white in the colocalization image.

smaller particles, due to their smaller size, are more efficient in penetrating the more narrow regions in the condensed chromatin. Therefore, they have access to a larger surface of the chromatin and can be anchored more easily e.g. when they are surrounded by chromatin in those grooves. For a given size, positively charged nanoparticles were most efficiently included in the nuclei, followed by the negatively charged or PEGylated ones, which can most likely be explained by aspecific interactions of the positively charged beads with the negatively charged chromatin. It should be noted that, for both the positively and negatively charged beads, interactions of the beads with poly-ions or proteins of the cytosolic extract, before nuclear reassembly starts, could influence the overall charge and nuclear inclusion of the beads. This could explain why the negatively charged beads are better included then the PEGylated ones, since the inert PEG chains lack the possibility to interact with the cytosolic poly-ions, proteins or chromatin material during the reassembly reaction, although the PEGylated beads also possessed a slightly negative charge (see Table 1). Furthermore, we were able to demonstrate that nanoparticles or pDNA/PEI complexes which are targeted to the chromatin have about 2−3 times higher probability of being retained in the artificial nuclei. However, not all the particles which were first bound to the chromatin were finally included in the nuclei. Most likely, adding the membrane fraction, which is the next step in the XNER assay, results in competition for binding to the chromatin, causing the majority of chromatin-bound nanoparticles (purple bars in Figure 5) to dissociate from the chromatin when the nuclear membrane formation proceeds. Figure 5 shows that a higher number of pDNA/PEI complexes are enclosed in the artificial nuclei when compared to polystyrene beads. This can be the result of multiple factors. We believe this can be related to the heterogeneity of the pDNA/PEI complexes, which can influence the charge distribution on their surface, the size and the shape of the complexes. The resulting larger surface or charge density is expected to give rise to more effective binding and therefore inclusion of the complexes to a larger extent. Additionally, it is not unlikely that the presence of DNA itself accounts for a great deal for the differences observed between the pDNA/PEI complexes and the polystyrene beads. Partially exposed DNA in the pDNA/PEI complexes could for example be anchored to the chromatin through the interaction with DNA binding proteins.

Based on these observations in the XNER assay, we conclude that it should be possible to bring nanoparticles into the nuclei of dividing cells, providing that they are not too large and are able to bind to the chromatin either by their intrinsic positive charge or through the use of chromatin binding peptides. However, unlike with the XNER assay, nuclear inclusion in dividing HeLa cells was never observed. Instead, the nanoparticles accumulated in a perinuclear region, which corresponds to the lysosomal compartment as evidenced by colocalization experiments. Two hypotheses could explain the lack of nuclear inclusion and the specific perinuclear distribution observed in living cells: (1) the nanoparticles are trafficked to the perinuclear region even before cell division occurs and are therefore not free but separated from the chromatin during cell division or (2) the nanoparticles are included in the nuclei during cell division but are expelled from the nuclei and subsequently accumulate in the perinuclear region. To examine these hypotheses, extensive, detailed real-time analysis of the intracellular distribution of the microinjected nanoparticles would be needed. The first hypothesis is favored by the observation that the nanoparticles are present in the perinuclear region where typically also lysosomes and endosomal vesicles accumulate. This would imply that, after microinjection,

the foreign nanoparticles are recognized by the endosomal machinery and are entrapped in lysosomal vesicles which traffic to the perinuclear region and physically separate the nanoparticles from the chromatin during cell division. Nativo and colleagues also detected that a large population of one of their modified gold nanoparticles groups in the vicinity of the nucleus. They stated these were associated with damaged or aberrant endosomes.[48] In relation to recent studies which indicate that nanoparticles are potent autophagy activators, the vesicles we observe can be part of cytoplasmic secretion, exocytosis or autophagy, a process by which the cell recycles and subsequently degrades its own components and clears itself of nanoparticles.[49] Chithrani and colleagues showed that nanoparticles about to be removed from cells appeared to be localized in late endosomes and lysosomes.[27] Also, this could explain the differences between the observations in the XNER assay and living cells, since in cell-free systems, mitotic spindles are totally absent and the influence of endocytosis/autophagy cannot be studied. This shows that we should not assume that results obtained from cell-free studies will all apply to living cells, in which additional barriers have to be taken into account.[41,50] We do believe, however, that the XNER assay is a valuable platform for testing "new" chromatin or nuclear targeting vehicles, because it isolates the nuclear envelope reassembly without the influence of other barriers such as cellular uptake or endosomal escape.

The second hypothesis would imply that the nanoparticles can bind the chromatin, but that there is a mechanism which is able to remove the nanoparticles again so that they are not included in the maturated nuclei. Or the chromatin binding is not strong enough to hold the "big" nanoparticles or there must be a yet unknown "eliminating" mechanism. Ludtke et al. and Swanson et al. showed that, after cytoplasmic delivery by microinjection or scratch-loading, the bulk of labeled pDNA or dextran (>40 kDa) remained cytoplasmic regardless of cell division. After nuclear injection, however, the labeled pDNA or dextran (>40 kDa) was nuclear in undivided cells, but mainly cytoplasmic in divided cells,[51,52] supporting the idea that only the chromosomes themselves and macromolecules physically associated with them were included in the newly formed nuclei.[52,53] They did not mention the possibility that the macromolecules can be inside immature nuclei and can be excluded later. In contrast, Gasiorowski and Dean have shown that naked, unmodified pDNA microinjected directly into the nucleus was able to partition evenly to the two daughter nuclei, but that this postmitotic nuclear retention was altered by DNA labeling methods, resulting in nuclear exclusion of labeled pDNA, while nonmodified pDNA was retained.[54] In this study, we cannot exclude that the labeling of our pDNA has an influence on the nuclear exclusion of our pDNA/PEI polyplexes. It should be noted, however, that in our study the labeled pDNA is mainly present in the core of the pDNA/PEI polyplexes and is therefore not expected to significantly alter the intracellular behavior of these particles. Also in the case of the labeled polystyrene beads the fluorophores are present inside the core of the nanoparticles, and this is not expected to influence the intracellular distribution of these beads.

In summary, although nuclear inclusion was observed in the XNER assay, we hypothesize that in living cells the nanoparticles are either intracellularly "trapped" in vesicles and are thus not free to bind to the chromatin, or do indeed enter the nuclei of dividing cells, but are again expelled and then accumulate in the lysosomal compartment. The nature of the mechanism that prevents the nuclear inclusion of nanoparticles in living HeLa cells is a topic that requires further study. It is, however, an interesting observation that nanoparticles which were injected in the cytoplasm of cells end up in the lysosomal compartment, even when they are not taken up by endocytosis. This implies the possibility to "endocytose" nanoparticles which are free in the cytosol, a mechanism which requires further investigation as this is highly relevant toward all sorts of gene delivery vehicles. We do believe, however, that nuclear inclusion should be possible when the nanoparticles are free in the cytoplasm at the onset of cell division. Also, as the XNER assay demonstrated, anchoring the nanoparticles to the chromatin by chromatin targeting peptides could help to improve the nuclear inclusion. This makes it an attractive future strategy for nonviral gene delivery, providing that other intracellular barriers such as the entrapment in the lysosomal compartment are first overcome.

AUTHOR INFORMATION

Corresponding Author

*Faculty of Pharmaceutical Sciences, Ghent University, Lab General Biochemistry & Physical Pharmacy, Harelbekestraat 72, 9000 Ghent, Belgium. E-mail: Katrien.Remaut@UGent.be. Phone: +32 9 264 80 47. Fax: +32 9 264 81 89.

ACKNOWLEDGMENT

N.S. is a predoctoral fellow from the Agency for Innovation through Science and Technology in Flanders (IWT). K.R. is a postdoctoral fellow of the Research Foundation Flanders (FWO). The financial support of these institutes and of EMBL is acknowledged with gratitude.

REFERENCES

(1) Mountain, A. Gene therapy: the first decade. *Trends Biotechnol.* **2000**, *18* (3), 119–128.

(2) Dowty, M. E.; Williams, P.; Zhang, G. F.; Hagstrom, J. E.; Wolff, J. A. Plasmid DNA Entry into Postmitotic Nuclei of Primary Rat Myotubes. *Proc. Natl. Acad. Sci. U.S.A.* **1995**, *92* (10), 4572–4576.

(3) Capecchi, M. R. High efficiency transformation by direct microinjection of DNA into cultured mammalian cells. *Cell* **1980**, *22* (2 Pt 2), 479–488.

(4) Lechardeur, D.; Sohn, K. J.; Haardt, M.; Joshi, P. B.; Monck, M.; Graham, R. W.; Beatty, B.; Squire, J.; O'Brodovich, H.; Lukacs, G. L. Metabolic instability of plasmid DNA in the cytosol: a potential barrier to gene transfer. *Gene Ther.* **1999**, *6* (4), 482–497.

(5) Xu, Y.; Szoka, F. C., Jr. Mechanism of DNA release from cationic liposome/DNA complexes used in cell transfection. *Biochemistry* **1996**, *35* (18), 5616–5623.

(6) Lechardeur, D.; Lukacs, G. L. Nucleocytoplasmic transport of plasmid DNA: A perilous journey from the cytoplasm to the nucleus. *Hum. Gene Ther.* **2006**, *17* (9), 882–889.

(7) Mirzayans, R.; Aubin, R. A.; Paterson, M. C. Differential expression and stability of foreign genes introduced into human fibroblasts by nuclear versus cytoplasmic microinjection. *Mutat. Res.* **1992**, *281* (2), 115–122.

(8) Mannisto, M.; Ronkko, S.; Matto, M.; Honkakoski, P.; Hyttinen, M.; Pelkonen, J.; Urtti, A. The role of cell cycle on polyplex-mediated gene transfer into a retinal pigment epithelial cell line. *J. Gene Med.* **2005**, *7* (4), 466–476.

(9) Escriou, V.; Carriere, M.; Bussone, F.; Wils, P.; Scherman, D. Critical assessment of the nuclear import of plasmid during cationic lipid-mediated gene transfer. *J. Gene Med.* **2001**, *3* (2), 179–187.

(10) Matsui, H.; Johnson, L. G.; Randell, S. H.; Boucher, R. C. Loss of binding and entry of liposome-DNA complexes decreases transfection

efficiency in differentiated airway epithelial cells. *J. Biol. Chem.* **1997**, *272* (2), 1117–1126.

(11) Fasbender, A.; Zabner, J.; Zeiher, B. G.; Welsh, M. J. A low rate of cell proliferation and reduced DNA uptake limit cationic lipid-mediated gene transfer to primary cultures of ciliated human airway epithelia. *Gene Ther.* **1997**, *4* (11), 1173–1180.

(12) Collas, P.; Husebye, H.; Alestrom, P. The nuclear localization sequence of the SV40 T antigen promotes transgene uptake and expression in zebrafish embryo nuclei. *Transgenic Res.* **1996**, *5* (6), 451–458.

(13) Sebestyen, M. G.; Ludtke, J. J.; Bassik, M. C.; Zhang, G.; Budker, V.; Lukhtanov, E. A.; Hagstrom, J. E.; Wolff, J. A. DNA vector chemistry: the covalent attachment of signal peptides to plasmid DNA. *Nat. Biotechnol.* **1998**, *16* (1), 80–85.

(14) Chen, J.; Stickles, R. J.; Daichendt, K. A. Galactosylated histone-mediated gene transfer and expression. *Hum. Gene Ther.* **1994**, *5* (4), 429–435.

(15) Mistry, A. R.; Falciola, L.; Monaco, L.; Tagliabue, R.; Acerbis, G.; Knight, A.; Harbottle, R. P.; Soria, M.; Bianchi, M. E.; Coutelle, C.; Hart, S. L. Recombinant HMG1 protein produced in Pichia pastoris: a nonviral gene delivery agent. *BioTechniques* **1997**, *22* (4), 718–729.

(16) Dean, D. A. Import of plasmid DNA into the nucleus is sequence specific. *Exp. Cell Res.* **1997**, *230* (2), 293–302.

(17) Mortimer, I.; Tam, P.; MacLachlan, I.; Graham, R. W.; Saravolac, E. G.; Joshi, P. B. Cationic lipid-mediated transfection of cells in culture requires mitotic activity. *Gene Ther.* **1999**, *6* (3), 403–411.

(18) Wilke, M.; Fortunati, E.; vandenBroek, M.; Hoogeveen, A. T.; Scholte, B. J. Efficacy of a peptide-based gene delivery system depends on mitotic activity. *Gene Ther.* **1996**, *3* (12), 1133–1142.

(19) Brunner, S.; Sauer, T.; Carotta, S.; Cotten, M.; Saltik, M.; Wagner, E. Cell cycle dependence of gene transfer by lipoplex polyplex and recombinant adenovirus. *Gene Ther.* **2000**, *7* (5), 401–407.

(20) Jiang, C.; O'Connor, S. P.; Fang, S. L.; Wang, K. X.; Marshall, J.; Williams, J. L.; Wilburn, B.; Echelard, Y.; Cheng, S. H. Efficiency of cationic lipid-mediated transfection of polarized and differentiated airway epithelial cells in vitro and in vivo. *Hum. Gene Ther.* **1998**, *9* (11), 1531–1542.

(21) Tseng, W. C.; Haselton, F. R.; Giorgio, T. D. Mitosis enhances transgene expression of plasmid delivered by cationic liposomes. *Biochim. Biophys. Acta, Gene Struct. Expression* **1999**, *1445* (1), 53–64.

(22) Mannisto, M.; Reinisalo, M.; Ruponen, M.; Honkakoski, P.; Tammi, M.; Urtti, A. Polyplex-mediated gene transfer and cell cycle: effect of carrier on cellular uptake and intracellular kinetics, and significance of glycosaminoglycans. *J. Gene Med.* **2007**, *9* (6), 479–487.

(23) Nicolau, C.; Sene, C.; Liposome-Mediated, D. N. A. Transfer in Eukaryotic Cells - Dependence of the Transfer Efficiency Upon the Type of Liposomes Used and the Host-Cell Cycle Stage. *Biochim. Biophys. Acta* **1982**, *721* (2), 185–190.

(24) Oudrhiri, N.; Vigneron, J. P.; Peuchmaur, M.; Leclerc, T.; Lehn, J. M.; Lehn, P. Gene transfer by guanidinium-cholesterol cationic lipids into airway epithelial cells in vitro and in vivo. *Proc. Natl. Acad. Sci. U.S.A.* **1997**, *94* (5), 1651–1656.

(25) Feldherr, C. M. Nucleocytoplasmic exchanges during cell division. *J. Cell Biol.* **1966**, *31* (1), 199–203.

(26) Rejman, J.; Oberle, V.; Zuhorn, I. S.; Hoekstra, D. Size-dependent internalization of particles via the pathways of clathrin- and caveolae-mediated endocytosis. *Biochem. J.* **2004**, *377* (Pt 1), 159–69.

(27) Chithrani, B. D.; Chan, W. C. Elucidating the mechanism of cellular uptake and removal of protein-coated gold nanoparticles of different sizes and shapes. *Nano Lett.* **2007**, *7* (6), 1542–50.

(28) Pan, Y.; Neuss, S.; Leifert, A.; Fischler, M.; Wen, F.; Simon, U.; Schmid, G.; Brandau, W.; Jahnen-Dechent, W. Size-dependent cytotoxicity of gold nanoparticles. *Small* **2007**, *3* (11), 1941–9.

(29) Errington, R. J.; Brown, M. R.; Silvestre, O. F.; Njoh, K. L.; Chappell, S. C.; Khan, I. A.; Rees, P.; Wilks, S. P.; Smith, P. J.; Summers, H. D. Single cell nanoparticle tracking to model cell cycle dynamics and compartmental inheritance. *Cell Cycle* **2010**, *9* (1), 121–130.

(30) Peeters, L.; Sanders, N. N.; Braeckmans, K.; Boussery, K.; Van de Voorde, J.; De Smedt, S. C.; Demeester, J. Vitreous: a barrier to nonviral ocular gene therapy. *Invest. Ophthalmol. Visual Sci.* **2005**, *46* (10), 3553–3561.

(31) Franz, C.; Walczak, R.; Yavuz, S.; Santarella, R.; Gentzel, M.; Askjaer, P.; Galy, V.; Hetzer, M.; Mattaj, I. W.; Antonin, W. MEL-28/ELYS is required for the recruitment of nucleoporins to chromatin and postmitotic nuclear pore complex assembly. *EMBO Rep.* **2007**, *8* (2), 165–72.

(32) Hetzer, M.; Bilbao-Cortes, D.; Walther, T. C.; Gruss, O. J.; Mattaj, I. W. GTP hydrolysis by Ran is required for nuclear envelope assembly. *Mol. Cell* **2000**, *5* (6), 1013–1024.

(33) Breuzard, G.; Tertil, M.; Goncalves, C.; Cheradame, H.; Geguan, P.; Pichon, C.; Midoux, P. Nuclear delivery of NFkappaB-assisted DNA/polymer complexes: plasmid DNA quantitation by confocal laser scanning microscopy and evidence of nuclear polyplexes by FRET imaging. *Nucleic Acids Res.* **2008**, *36* (12), e71.

(34) Aravind, L.; Landsman, D. AT-hook motifs identified in a wide variety of DNA-binding proteins. *Nucleic Acids Res.* **1998**, *26* (19), 4413–4421.

(35) Gunsalus, K. C.; Ge, H.; Schetter, A. J.; Goldberg, D. S.; Han, J. D.; Hao, T.; Berriz, G. F.; Bertin, N.; Huang, J.; Chuang, L. S.; Li, N.; Mani, R.; Hyman, A. A.; Sonnichsen, B.; Echeverri, C. J.; Roth, F. P.; Vidal, M.; Piano, F. Predictive models of molecular machines involved in Caenorhabditis elegans early embryogenesis. *Nature* **2005**, *436* (7052), 861–865.

(36) Fernandez, A. G.; Piano, F. MEL-28 is downstream of the Ran cycle and is required for nuclear-envelope function and chromatin maintenance. *Curr. Biol.* **2006**, *16* (17), 1757–1763.

(37) Zhou, X.; Benson, K. F.; Przybysz, K.; Liu, J.; Hou, Y.; Cherath, L.; Chada, K. Genomic structure and expression of the murine Hmgi-c gene. *Nucleic Acids Res.* **1996**, *24* (20), 4071–4077.

(38) Catez, F.; Yang, H.; Tracey, K. J.; Reeves, R.; Misteli, T.; Bustin, M. Network of dynamic interactions between histone H1 and high-mobility-group proteins in chromatin. *Mol. Cell. Biol.* **2004**, *24* (10), 4321–4328.

(39) Bianchi, M. E.; Agresti, A. HMG proteins: dynamic players in gene regulation and differentiation. *Curr. Opin. Genet. Dev.* **2005**, *15* (5), 496–506.

(40) Lohka, M. J.; Masui, Y. Roles of Cytosol and Cytoplasmic Particles in Nuclear-Envelope Assembly and Sperm Pronuclear Formation in Cell-Free Preparations from Amphibian Eggs. *J. Cell Biol.* **1984**, *98* (4), 1222–1230.

(41) Lohka, M. J.; Masui, Y. Formation in vitro of sperm pronuclei and mitotic chromosomes induced by amphibian ooplasmic components. *Science (New York, N.Y.)* **1983**, *220* (4598), 719–721.

(42) Laskey, R. A.; Mills, A. D.; Philpott, A.; Leno, G. H.; Dilworth, S. M.; Dingwall, C. The role of nucleoplasmin in chromatin assembly and disassembly. *Philos. Trans. R. Soc. London* **1993**, *339* (1289), 263–269discussion 268—269.

(43) Philpott, A.; Leno, G. H. Nucleoplasmin remodels sperm chromatin in Xenopus egg extracts. *Cell* **1992**, *69* (5), 759–767.

(44) Philpott, A.; Leno, G. H.; Laskey, R. A. Sperm Decondensation in Xenopus Egg Cytoplasm Is Mediated by Nucleoplasmin. *Cell* **1991**, *65* (4), 569–578.

(45) Newport, J.; Dunphy, W. Characterization of the Membrane-Binding and Fusion Events during Nuclear-Envelope Assembly Using Purified Components. *J. Cell Biol.* **1992**, *116* (2), 295–306.

(46) Gant, T. M.; Wilson, K. L. Nuclear assembly. *Annu. Rev. Cell Dev. Biol.* **1997**, *13*, 669–695.

(47) Summers, H. Can cells reduce nanoparticle toxicity? *Nano Today* **2010**, *5* (2), 83–84.

(48) Nativo, P.; Prior, I. A.; Brust, M. Uptake and intracellular fate of surface-modified gold nanoparticles. *ACS Nano* **2008**, *2* (8), 1639–1644.

(49) Seleverstov, O.; Phang, J. M.; Zabirnyk, O. Semiconductor nanocrystals in autophagy research: methodology improvement at nanosized scale. *Methods Enzymol.* **2009**, *452*, 277–296.

(50) Newport, J.; Spann, T. Disassembly of the nucleus in mitotic extracts: membrane vesicularization, lamin disassembly, and chromosome condensation are independent processes. *Cell* **1987**, *48* (2), 219–230.

(51) Ludtke, J. J.; Sebestyen, M. G.; Wolff, J. A. The effect of cell division on the cellular dynamics of microinjected DNA and dextran. *Mol. Ther.* **2002**, *5* (5), 579–588.

(52) Swanson, J. A.; McNeil, P. L. Nuclear reassembly excludes large macromolecules. *Science (New York, N.Y.)* **1987**, *238* (4826), 548–550.

(53) Benavente, R.; Scheer, U.; Chaly, N. Nucleocytoplasmic sorting of macromolecules following mitosis: fate of nuclear constituents after inhibition of pore complex function. *Eur. J. Cell Biol.* **1989**, *50* (1), 209–219.

(54) Gasiorowski, J. Z.; Dean, D. A. Postmitotic nuclear retention of episomal plasmids is altered by DNA labeling and detection methods. *Mol. Ther.* **2005**, *12* (3), 460–467.